Pt-decorated graphitic carbon nitride on carbon paper by x-ray photoelectron spectroscopy

Special Collection: Materials for Energy and the Environment

Mattia Brugia ; Alberto Gasparotto ; Mattia Benedet ; Davide Barreca ; Gian Andrea Rizzi ✉ ; Chiara Maccato

Check for updates

View Online

Export Citation

Pt-decorated graphitic carbon nitride on carbon paper by x-ray photoelectron spectroscopy

Mattia Brugia,[1,a)] Alberto Gasparotto,[1,2] Mattia Benedet,[1,2] Davide Barreca,[2] Gian Andrea Rizzi,[1,2,b)] and Chiara Maccato[1,2]

AFFILIATIONS

[1]Department of Chemical Sciences, Padova University and INSTM, 35131 Padova, Italy
[2]CNR-ICMATE and INSTM, Department of Chemical Sciences, Padova University, 35131 Padova, Italy

Note: This paper is part of the 2024 Special Topic Collection on Materials for Energy and the Environment.
[a)]**Electronic mail:** mattia.brugia@unipd.it
[b)]**Author to whom correspondence should be addressed:** gianandrea.rizzi@unipd.it

ABSTRACT

Nanocomposites based on Pt nanoparticles (NPs) and graphitic carbon nitride (gCN) have emerged as promising (photo)electrocatalysts for sustainable energy production, thanks to the synergistical combination of Pt NPs catalytic performances with the favorable gCN chemico-physical properties. In this work, we have focused on electrophoretic deposition of graphitic carbon nitride on carbon paper and subsequent system functionalization with Pt NPs by means of radio frequency sputtering under mild conditions. A final thermal treatment was performed both in air and under inert atmospheres to assess its influence on Pt oxidation states and the related interplay with ultimate functional performances. The present study is focused on x-ray photoelectron spectroscopy characterization of two representative gCN-Pt nanocomposite specimens, annealed in Ar and in air. In particular, we report the survey spectra and the detailed scans for C 1s, N 1s, O 1s, and Pt 4f regions, analyzing the principal spectral features and comparatively discussing the resulting material properties.

INTRODUCTION

Graphitic carbon nitride (gCN), the most stable phase of carbon nitride polymorphs under ambient conditions, is a fascinating nontoxic polymeric semiconductor possessing a good visible light response for wavelengths <455 nm, corresponding to a bandgap of ≈2.7 eV (Refs. 1–3). Over the last decade, gCN-based systems have attracted an enormous attention as metal-free, multipurpose photocatalysts for pollutant degradation and clean energy generation (Refs. 1–7). These applications rely on the unique set of gCN optical, electronic, and chemical characteristics, combined with its facile synthesis from readily available precursors, and its stability even in adverse chemical and physical environments

(Refs. 5, 8, and 9). Nevertheless, these gCN advantages are at least partially eclipsed by some shortcomings, including the limited active area and the rapid recombination of photogenerated charge carriers (Refs. 6, 10, and 11). In the framework of the various research activities aimed at alleviating these problems and boosting the system performances (Refs. 1, 2, 6, 12, and 13), valuable strategies consist in nanostructure design, to attain a larger specific surface area (Refs. 10 and 14), as well as in the introduction of nanodispersed metal or metal oxide co-catalysts (Refs. 9, 11, 15, and 16). In fact, graphitic carbon nitride is endowed with abundant reactive sites for the construction of metal/gCN hybrids, in which gCN can act not only as template but also as a photoactive support

for anchoring metal nanostructures (Refs. 3, 8, 17, and 18). The corresponding heterojunction formation can favorably extend the lifetime of electron/hole pairs and limit recombination losses, thus promoting an increase in material catalytic activity (Ref. 17). In this context, platinum nanoparticles represent an attractive choice as metal functionalizing agents in the manufacturing of various functional nanocomposites (Refs. 2, 8, 9, 14, and 17–25).

In general, deposition of noble metal nanoparticles on gCN can be performed by different methods, encompassing chemical or microwave-assisted reduction, photodeposition, and electrochemical synthesis (Refs. 9 and 14). The resulting nanoparticles typically have mean sizes of several nanometers and are prone to aggregation phenomena, leading to a decrease in surface active sites that detrimentally affect the system performances (Ref. 21). In a different way, the use of low-temperature plasmas for metal nanoparticles (NPs) introduction represents an energy-efficient nanofabrication tool for the ultrafine dispersion of NPs, ultimately affording a higher material photoactivity (Ref. 9).

In the course of our activities on gCN-containing nanostructures as photoelectrocatalysts for the oxygen evolution reaction (Refs. 15 and 16), we have successfully fabricated composite systems containing ultradispersed metal or metal oxide-based co-catalysts by the initial liquid-phase gCN preparation, followed by radio frequency (RF) sputtering from nonequilibrium plasmas at low temperatures. Following an analogous strategy, in the present work, Pt-gCN nanocomposites were prepared by the initial electrophoretic deposition (EPD) of gCN on carbon paper (CP), followed by platinum sputtering from Ar plasmas under optimized conditions. An ultimate thermal treatment was, hence, performed either in air or under Ar. In this study, we present a detailed comparative x-ray photoelectron spectroscopy (XPS) characterization of the resulting systems, showing that the mutual content of oxidized Pt species is directly dependent on adopted annealing conditions. The critical discussion of the results provided herein may serve as a useful reference guide for additional studies on homologous materials and also support the interpretation of material structure-property interplay in view of various photocatalytic and electrocatalytic end-uses.

SPECIMEN DESCRIPTION [ACCESSION # 01959]

Specimen: gCN-Pt, annealed in Ar

CAS Registry #: Unknown

Specimen Characteristics: Homogeneous; solid; polycrystalline; semiconductor; composite; thin film

Chemical Name: Graphitic carbon nitride-platinum

Source: Specimen prepared by gCN electrophoretic deposition on carbon paper, followed by platinum sputtering for 60 min and final thermal treatment in Ar at 400 °C for 2.5 h.

Composition: C, N, O, and Pt

Form: Supported nanocomposite

Structure: X-ray diffraction (XRD) analysis evidenced one intense reflection at $2\theta \approx 26.4°$ and minor peaks at $\approx 42.4°$, 44.5°, and 54.5°, respectively, ascribed to (002), (100), (101), and (404) crystallographic planes of graphite from the CP support (ICDD PDF #08-0415). Fourier-transform infrared (FT-IR) spectroscopy analysis revealed the typical vibrational modes of the gCN network in

the 1200–1700 cm^{-1} range (Ref. 1), a peak at 810 cm^{-1} due to out-of-plane bending of heptazinic rings (Ref. 4), and a broad band at 3200–3300 cm^{-1} due to the presence of uncondensed $-NH_x$ groups (x = 1 and 2) and chemisorbed $-OH/H_2O$ (Refs. 5 and 10). Scanning electron microscopy (SEM) analyses (see the inset in figure accession # **01959-01**) evidenced that the gCN deposit was characterized by a rounded and globular morphology covering the underlying CP and was uniformly decorated by Pt-based nanoparticles (mean size ≈ 8.3 nm).

History and Significance: gCN powders were synthesized by thermal condensation of the cyanuric acid–melamine supramolecular complex (CM complex; see Ref. 15). The obtained powders were used as precursors for gCN deposition on precleaned carbon paper substrates (P50, AvCarb®; 150 μm thickness, $\approx 1 \times 1$ cm^2 area) by EPD. Depositions were carried out by applying a potential of 10 V for an overall duration of 30 s, following a previous work (Ref. 12). The obtained sample was annealed at 400 °C for 2.5 h under flowing Ar. The subsequent functionalization with Pt was performed by RF sputtering ($\nu = 13.56$ MHz) from an Ar plasma in a custom-built two-electrode reactor. A Pt target (Alfa Aesar, 99%; thickness = 0.3 mm) was fixed on the RF electrode, while carbon paper-supported gCN samples were mounted on the grounded one. According to a previous work (Ref. 26), depositions were performed using the following settings: electronic grade Ar flow rate = 10 standard cubic centimeters per minute (SCCM); total pressure = 0.30 mbar; RF power = 5 W; sputtering time = 60 min; and growth temperature = 60 °C. Finally, thermal treatment was carried out at 400 °C for 2.5 h under flowing Ar.

As Received Condition: As grown

Analyzed Region: Same as the host material

***Ex Situ* Preparation/Mounting:** Sample fixed by a metallic clip on a grounded sample holder and introduced into the analysis chamber through a fast entry system.

***In Situ* Preparation:** None

Charge Control: After fixing the carbon paper-supported sample to the sample holder with metallic clips, we observed charging problems upon spectra acquisition, evidently caused by an improper electrical contact between the carbon paper and the sample holder. As a consequence, all the spectra reported in this article have been acquired using charge compensation. The latter was performed by a dual-beam low-energy electron and ion coaxial flood source (0.1 V, 175 μA, and gas cell at 20 V).

Temp. During Analysis: 298 K

Pressure During Analysis: $<10^{-7}$ Pa

Pre-analysis Beam Exposure: 120 s

SPECIMEN DESCRIPTION (ACCESSION # 01960)

Specimen: gCN-Pt, annealed in air

CAS Registry #: Unknown

Specimen Characteristics: Homogeneous; solid; polycrystalline; semiconductor; composite; thin film

Chemical Name: Graphitic carbon nitride-platinum

Source: Specimen prepared by gCN electrophoretic deposition on carbon paper, followed by platinum sputtering for 60 min and final thermal treatment in air at 400 °C for 2.5 h.

Composition: C, N, O, and Pt

Form: Supported nanocomposite

Structure: The XRD and FT-IR analyses yielded results analogous to the specimen described in accession # **01959**. SEM analyses (see the inset in figure accession # **01960-01**) evidenced a similar morphology for gCN that was evenly decorated by Pt-based nanoparticles (average dimensions of ≈7.9 nm).

History and Significance: Synthesis, deposition, and functionalization conditions were the same described for the previous specimen. The only difference was the final thermal treatment, carried out at 400 °C for 2.5 h in open air.

As Received Condition: As grown

Analyzed Region: Same as the host material

Ex Situ **Preparation/Mounting:** Sample fixed by a metallic clip on a grounded sample holder and introduced into the analysis chamber through a fast entry system.

In Situ **Preparation:** None

Charge Control: Charge compensation was performed by a dual-beam low-energy electron and ion coaxial flood source (0.1 V, 175 μA, and gas cell at 20 V).

Temp. During Analysis: 298 K

Pressure During Analysis: $<10^{-7}$ Pa

Pre-analysis Beam Exposure: 120 s

INSTRUMENT DESCRIPTION

Manufacturer and Model: ThermoFisher Scientific Escalab^{TM} QXi

Analyzer Type: Spherical sector

Detector: Channeltron

Number of Detector Elements: 6

INSTRUMENT PARAMETERS COMMON TO ALL SPECTRA

Spectrometer

Analyzer Mode: Constant pass energy

Throughput (T = E^N): The transmission function is calculated from a cubic polynomial fit to a plot of log[peak area/(PE × XSF)] versus log(KE/PE), where PE is the pass energy, KE is the kinetic energy, and XSF is the relative sensitivity factor (Refs. 27 and 28).

Excitation Source Window: None

Excitation Source: Al K_α monochromatic

Source Energy: 1486.6 eV

Source Strength: 200 W

Source Beam Size: $500 \times 500\,\mu$m^2

Signal Mode: Single channel direct

Geometry

Incident Angle: 58°

Source-to-Analyzer Angle: 58°

Emission Angle: 0°

Specimen Azimuthal Angle: 90°

Acceptance Angle from Analyzer Axis: 45°

Analyzer Angular Acceptance Width: 22.5° × 22.5°

Ion Gun

Manufacturer and Model: ThermoFisher Scientific MAGCIS Dual Beam Ion Source

Energy: 4000 eV

Current: 7 mA

Current Measurement Method: Biased stage

Sputtering Species and Charge: Ar$^+$

Spot Size (unrastered): 500 μm

Raster Size: $4500 \times 4500\,\mu$m^2

Incident Angle: 40°

Polar Angle: 40°

Azimuthal Angle: 270°

Comment: Differentially pumped ion gun

DATA ANALYSIS METHOD

Energy Scale Correction: The reported binding energies were corrected for charging phenomena by assigning a BE of 284.8 eV to the adventitious C 1s signal (Refs. 27 and 28).

Recommended Energy Scale Shift: +0.78 eV for accession # **01959** and +0.82 eV for accession # **01960.**

Peak Shape and Background Method: In this work, peak fitting was carried out with utmost care to avoid any major source of significant errors (Ref. 29). In particular, after Shirley-type background subtraction (Ref. 30), least-squares fitting was performed using XPSPEAK software (version 4.1) (Ref. 31), adopting Gaussian/Lorentzian sum functions (typical mixing parameter = 0.2–0.3) (Ref. 32). Doniach–Sunjic functions were used for the fitting of Pt(0) contributions to the Pt 4f photoelectron signals. Asymmetric peaks were also used for the sp^2 C 1s low BE components at 284.2 eV.

Quantitation Method: Relative quantification was accomplished by normalizing peak areas for the respective sensitivity factors (Ref. 33). The sensitivity factors used in this work have been provided by Thermo Scientific Avantage software (version 6.6.0, Build 00114). The involved calculations were carried out using a smart Shirley function for the background, which implements an additional constraint to ensure the background intensity is not higher than the actual data at any point in the region (Refs. 27 and 28).

AUTHOR DECLARATIONS

Conflict of Interest

The authors have no conflicts to disclose.

Author Contributions

Mattia Brugia: Investigation (equal); Software (equal); Validation (equal); Visualization (equal); Writing – review & editing (equal). **Alberto Gasparotto:** Data curation (equal); Formal analysis (lead); Funding acquisition (equal); Investigation (equal); Methodology (equal); Writing – original draft (lead). **Mattia Benedet:** Data curation (equal); Methodology (equal); Validation (equal); Visualization (equal). **Davide Barreca:** Conceptualization (equal); Formal analysis (equal); Funding acquisition (equal); Supervision (equal); Writing – review & editing (equal). **Gian Andrea Rizzi:** Data curation (equal); Funding acquisition (equal); Investigation (equal); Visualization (equal); Writing – review & editing (equal). **Chiara Maccato:** Formal analysis (equal); Funding acquisition (lead); Methodology (equal); Supervision (equal); Visualization (equal); Writing – review & editing (equal).

DATA AVAILABILITY

The data that support the findings of this study are available within the article and its supplementary material.

REFERENCES

[1]K. Wang, Q. Li, B. Liu, B. Cheng, W. Ho, and J. Yu, Appl. Catal. B **176–177**, 44 (2015).
[2]J. Yu, K. Wang, W. Xiao, and B. Cheng, Phys. Chem. Chem. Phys. **16**, 11492 (2014).
[3]C. Han, L. Du, M. Konarova, D.-C. Qi, D. L. Phillips, and J. Xu, ACS Catal. **10**, 9227 (2020).
[4]X. Yuan, K. Luo, K. Zhang, J. He, Y. Zhao, and D. Yu, J. Phys. Chem. A **120**, 7427 (2016).
[5]T. S. Miller, A. B. Jorge, T. M. Suter, A. Sella, F. Corà, and P. F. McMillan, Phys. Chem. Chem. Phys. **19**, 15613 (2017).
[6]P. Qiu, C. Xu, H. Chen, F. Jiang, X. Wang, R. Lu, and X. Zhang, Appl. Catal. B **206**, 319 (2017).
[7]T. Ma, J. Bai, and C. Li, Vacuum **145**, 47 (2017).
[8]M. Zhu, C. Zhai, M. Sun, Y. Hu, B. Yan, and Y. Du, Appl. Catal. B **203**, 108 (2017).
[9]J. Ding *et al.*, J. Alloys Compd. **873**, 159871 (2021).
[10]Y. Xiao, G. Tian, W. Li, Y. Xie, B. Jiang, C. Tian, D. Zhao, and H. Fu, J. Am. Chem. Soc. **141**, 2508 (2019).
[11]P. Qiu, H. Chen, and F. Jiang, RSC Adv. **4**, 39969 (2014).
[12]M. Benedet *et al.*, ACS Appl. Mater. Interfaces **15**, 47368 (2023).
[13]L. Lei, H. Fan, Y. Jia, X. Wu, Q. Zhong, and W. Wang, Appl. Surf. Sci. **606**, 154938 (2022).
[14]K. Li, Z. Zeng, L. Yan, S. Luo, X. Luo, M. Huo, and Y. Guo, Appl. Catal. B **165**, 428 (2015).
[15]M. Benedet, A. Gasparotto, G. A. Rizzi, D. Barreca, and C. Maccato, Surf. Sci. Spectra **29**, 024001 (2022).
[16]M. Benedet, G. A. Rizzi, D. Barreca, A. Gasparotto, and C. Maccato, Surf. Sci. Spectra **30**, 014004 (2023).
[17]M. Aksoy and Ö. Metin, ACS Appl. Nano Mater. **3**, 6836 (2020).
[18]K. S. Bhavani, T. Anusha, and P. K. Brahman, Int. J. Hydrogen Energy **46**, 9199 (2021).
[19]M. E. A. Warwick, K. Kaunisto, G. Carraro, A. Gasparotto, C. Maccato, and D. Barreca, Surf. Sci. Spectra **22**, 47 (2015).
[20]H. Huang, S. Yang, R. Vajtai, X. Wang, and P. M. Ajayan, Adv. Mater. **26**, 5160 (2014).
[21]M. Sadhukhan, M. K. Kundu, T. Bhowmik, and S. Barman, Int. J. Hydrogen Energy **42**, 9371 (2017).
[22]K. Ghosh, M. Kumar, H. Wang, T. Maruyama, and Y. Ando, J. Phys. Chem. C **114**, 5107 (2010).
[23]Z. Zeng *et al.*, Nano Energy **69**, 104409 (2020).
[24]W. Zhang, Y. Fu, J. Wang, and X. Wang, Adv. Mater. Interfaces **4**, 1601219 (2017).
[25]F. Su, C. K. Poh, J. Zeng, Z. Zhong, Z. Liu, and J. Lin, J. Power Sources **205**, 136 (2012).
[26]M. E. A. Warwick *et al.*, Phys. Chem. Chem. Phys. **17**, 12899 (2015).
[27]K. M. Cole, D. W. Kirk, and S. J. Thorpe, Surf. Sci. Spectra **28**, 014001 (2021).
[28]K. M. Cole, D. W. Kirk, and S. J. Thorpe, Surf. Sci. Spectra **27**, 024013 (2020).
[29]D. R. Baer, G. E. McGuire, K. Artyushkova, C. D. Easton, M. H. Engelhard, and A. G. Shard, J. Vac. Sci. Technol. A **39**, 021601 (2021).
[30]D. A. Shirley, Phys. Rev. B **5**, 4709 (1972).
[31]See: https://xpspeak.software.informer.com/4.1/.
[32]V. Jain, M. C. Biesinger, and M. R. Linford, Appl. Surf. Sci. **447**, 548 (2018).
[33]K. Berresheim, M. Mattern-Klosson, and M. Wilmers, Fresenius J. Anal. Chem. **341**, 121 (1991).
[34]See: http://srdata.nist.gov/xps.
[35]D. J. Morgan, C-J. Carbon Res. **7**, 51 (2021).
[36]I. Bertóti, M. Mohai, and K. László, Carbon **84**, 185 (2015).
[37]D. Lützenkirchen-Hecht, K. Rohrmann, T. Stöcker, and W. Thiel, Surf. Interface Anal. **39**, 845 (2007).
[38]J. F. Moulder, W. F. Stickle, P. E. Sobol, and K. D. Bomben, *Handbook of X-ray Photoelectron Spectroscopy* (Perkin Elmer Corporation, Eden Prairie, MN, 1992).

SPECTRAL FEATURES TABLE

Spectrum ID #	Element/ Transition	Peak Energy (eV)	Peak Width FWHM (eV)	Peak Area (eV counts/s)	Sensitivity Factor	Concentration (at. %)	Peak Assignment
01959-02[a]	C 1s	284.2	1.5	64 213.2	1.000	12.3	C sp^2 in carbon paper
01959-02[a]	C 1s	284.8	1.9	86 791.5	1.000	16.7	Adventitious surface contamination
01959-02[a]	C 1s	285.6	1.8	75 601.1	1.000	14.5	C in C—NH$_x$ (x = 1 and 2) groups on gCN edges and adsorbed carbonates
01959-02[a]	C 1s	288.3	2.0	98 014.8	1.000	18.8	N═C—N carbon atoms in gCN aromatic rings
01959-02[a]	C 1s	294.1	3.0	4 509.1	1.000	0.9	Excitation of π-electrons in gCN heptazinic rings
01959-03[b]	N 1s	398.6	1.8	124 738.3	1.676	14.3	Two-coordinated C═N—C nitrogen atoms in gCN
01959-03[b]	N 1s	399.9	1.7	40 051.7	1.676	4.6	Tertiary N—(C)$_3$ nitrogen atoms in gCN
01959-03[b]	N 1s	401.1	1.7	23 114.4	1.676	2.6	N in NH$_x$ (x = 1 and 2) uncondensed amino groups
01959-03[b]	N 1s	404.5	2.9	11 358.0	1.676	1.3	Excitation of π-electrons in gCN heptazinic rings
01959-04[c]	O 1s	531.5	2.4	29 078.8	2.881	1.9	Surface adsorbed hydroxyl/carbonate groups and PtO$_x$ (x = 1 and 2)
01959-04[c]	O 1s	533.2	2.6	38 389.4	2.881	2.6	Surface adsorbed water
01959-05[d]	Pt 4f	…	…	550 321.3	16.678	6.3	Pt(0)
01959-05[d]	Pt 4f$_{7/2}$	71.2	1.8	…	…	…	Pt(0)
01959-05[d]	Pt 4f$_{5/2}$	74.5	1.8	…	…	…	Pt(0)
01959-05[d]	Pt 4f	…	…	216 399.0	16.678	2.5	Pt(II) in PtO
01959-05[d]	Pt 4f$_{7/2}$	72.7	1.9	…	…	…	Pt(II) in PtO
01959-05[d]	Pt 4f$_{5/2}$	76.0	1.9	…	…	…	Pt(II) in PtO
01959-05[d]	Pt 4f	…	…	57 311.4	16.678	0.7	Pt(IV) in PtO$_2$
01959-05[d]	Pt 4f$_{7/2}$	74.6	2.7	…	…	…	Pt(IV) in PtO$_2$
01959-05[d]	Pt 4f$_{5/2}$	77.9	2.7	…	…	…	Pt(IV) in PtO$_2$
01960-02[a]	C 1s	284.2	1.4	15 976.9	1.000	2.8	C sp^2 in carbon paper
01960-02[a]	C 1s	284.8	1.6	56 238.8	1.000	9.9	Adventitious surface contamination
01960-02[a]	C 1s	285.2	1.6	122 702.9	1.000	21.7	C in C—NH$_x$ (x = 1 and 2) groups on gCN edges and adsorbed carbonates
01960-02[a]	C 1s	288.2	2.0	118 548.9	1.000	21.0	N═C—N carbon atoms in gCN aromatic rings
01960-02[a]	C 1s	294.1	3.0	6 071.2	1.000	1.1	Excitation of π-electrons in gCN heptazinic rings
01960-03[b]	N 1s	398.7	1.9	195 908.9	1.676	20.7	Two-coordinated C═N—C nitrogen atoms in gCN
01960-03[b]	N 1s	400.0	1.6	43 473.4	1.676	4.6	Tertiary N—(C)$_3$ nitrogen atoms in gCN
01960-03[b]	N 1s	401.0	1.6	28 424.9	1.676	3.0	N in NH$_x$ (x = 1 and 2) uncondensed amino groups
01960-03[b]	N 1s	404.9	2.9	25 191.9	1.676	1.1	Excitation of π-electrons in gCN heptazinic rings
01960-04[c]	O 1s	531.6	2.1	66 107.6	2.881	4.1	Surface adsorbed hydroxyl/carbonate groups and PtO$_x$ (x = 1 and 2)
01960-04[c]	O 1s	533.0	2.2	51 941.7	2.881	3.2	Surface adsorbed water
01960-05[d]	Pt 4f	…	…	213 162.6	16.678	2.3	Pt(0)

20 August 2024 12:16:47

SPECTRAL FEATURES TABLE (*Continued.*)

Spectrum ID #	Element/ Transition	Peak Energy (eV)	Peak Width FWHM (eV)	Peak Area (eV counts/s)	Sensitivity Factor	Concentration (at. %)	Peak Assignment
01960-05[d]	Pt $4f_{7/2}$	71.3	1.7	…	…	…	Pt(0)
01960-05[d]	Pt $4f_{5/2}$	74.7	1.7	…	…	…	Pt(0)
01960-05[d]	Pt $4f$	…	…	308 569.0	16.678	3.3	Pt(II) in PtO
01960-05[d]	Pt $4f_{7/2}$	72.5	2.2	…	…	…	Pt(II) in PtO
01960-05[d]	Pt $4f_{5/2}$	75.8	2.2	…	…	…	Pt(II) in PtO
01960-05[d]	Pt $4f$	…	…	124 215.7	16.678	1.3	Pt(IV) in PtO_2
01960-05[d]	Pt $4f_{7/2}$	74.3	2.2	…	…	…	Pt(IV) in PtO_2
01960-05[d]	Pt $4f_{5/2}$	77.5	2.2	…	…	…	Pt(IV) in PtO_2

[a]The sensitivity factor is referred to the whole C $1s$ signal.
[b]The sensitivity factor is referred to the whole N $1s$ signal.
[c]The sensitivity factor is referred to the whole O $1s$ signal.
[d]The sensitivity factor is referred to the whole Pt $4f$ signal.

Footnote to Spectra 01959-01 and 01960-01: Wide scan spectra presented the expected carbon and nitrogen signals along with the platinum ones, thus confirming the presence of gCN and its successful functionalization with Pt nanoparticles. The occurrence of oxygen is related to both chemisorbed species and platinum partial oxidation (see below).

Footnote to Spectra 01959-02 and 01960-02: For both specimens, five components contributed to the C $1s$ signal. The first one, centered at 284.2 eV, was attributed to the C sp^2 related to carbon paper support (Refs. 34 and 35), while the component at 284.8 eV arose from adventitious carbon contamination (Refs. 2, 8, 19, 34, and 36). The signal at BE ≈ 285.4 eV was attributed to C bonded to amino groups ($-NH_x$, x = 1 and 2), derived from an incomplete gCN thermal condensation (Ref. 17), and also to the presence of C—O—C and C—OH groups (Refs. 36 and 37) due to air and moisture exposure. The signal located at ≈288.3 eV was due to C atoms in N—C≡N moieties of the carbon nitride network (Refs. 13, 15, and 16). The last signal at 294.1 eV derived from π-electron excitations (Refs. 6 and 11).

Footnote to Spectra 01959-03 and 01960-03: The N $1s$ peak was fitted with four contributing bands. The signals located at ≈398.6 and ≈399.9 eV were attributed, respectively, to bi-coordinated (C═N—C) and tri-coordinated [N—(C)₃] N atoms in the gCN network (Refs. 2, 15, and 17). The peak at 401.0 eV was due to terminal $-NH_x$ groups (x = 1 and 2) (Refs. 8 and 9), whereas the signal of π electrons excitation appeared at 404.5 eV (Refs. 7 and 12).

Footnote to Spectra 01959-04 and 01960-04: For both samples, two components contributed to the O $1s$ photoelectron peak. The first one was centered at BE ≈ 531.6 eV and derived from surface-adsorbed hydroxyl and carbonate groups (Ref. 12) and also from O atoms in PtO_x (x = 1 and 2) (Refs. 9, 19, and 26). The other component at ≈533.1 eV was due to surface adsorbed water (Refs. 6, 14, 34, and 38).

Footnote to Spectra 01959-05 and 01960-05: For both specimens, the Pt $4f$ peak was fitted with three distinct doublets, corresponding to three diverse platinum chemical environments (Refs. 17, 19, 24, and 25). The predominant contribution, with Pt $4f_{7/2}$ BE ≈71.3 eV, was due to Pt(0) (Refs. 9, 18, 20, and 21). The second doublet (Pt $4f_{7/2}$ BE ≈ 72.6 eV) was derived from Pt(II) in PtO (Refs. 2, 3, 22, and 23). The last, higher BE doublet (Pt $4f_{7/2}$ BE≈74.5 eV) was attributed to Pt(IV) in PtO_2 (Refs. 19, 26, and 38). In the case of accession # **01959** (see 01959-05), Pt(0) was the predominant contribution, whereas oxidized Pt was mainly present as Pt(II). In a different way, for accession # **01960** (see 01960-05), Pt(II) became the main contribution and Pt(IV) amount significantly increased.

Overall, these results demonstrate the possibility of modulating the metal oxidation state in Pt-containing nanoparticles by a simple variation in the post-synthesis annealing atmosphere.

ANALYZER CALIBRATION TABLE

Spectrum ID #	Element/ Transition	Peak Energy (eV)	Peak Width FWHM (eV)	Peak Area (eV counts/s)	Sensitivity Factor	Concentration (at. %)	Peak Assignment
…	Au $4f_{7/2}$	84.0	1.1	2 841 305.7	20.735	…	Au(0)
…	Ag $3d_{5/2}$	368.3	0.9	1 316 206.9	22.131	…	Ag(0)
…	Cu $2p_{3/2}$	932.7	1.3	5 350 621.8	26.513	…	Cu(0)

**Comment to Analyzer Calibration Table:** The peaks were acquired after Ar⁺ erosion.

20 August 2024 12:16:47

GUIDE TO FIGURES

Spectrum (Accession) #	Spectral Region	Voltage Shift[a]	Multiplier	Baseline	Comment #
01959-01	Survey	−0.78	1	0	1
01959-02	C 1s	−0.78	1	0	1
01959-03	N 1s	−0.78	1	0	1
01959-04	O 1s	−0.78	1	0	1
01959-05	Pt 4f	−0.78	1	0	1
01960-01	Survey	−0.82	1	0	2
01960-02	C 1s	−0.82	1	0	2
01960-03	N 1s	−0.82	1	0	2
01960-04	O 1s	−0.82	1	0	2
01960-05	Pt 4f	−0.82	1	0	2

[a]Voltage shift of the archived (as-measured) spectrum relative to the printed figure. The figure reflects the recommended energy scale correction due to a calibration correction, sample charging, flood gun, or other phenomenon.

1. **gCN-Pt Ar**, annealed in Ar.
2. **gCN-Pt air**, annealed in air.

20 August 2024 12:16:47
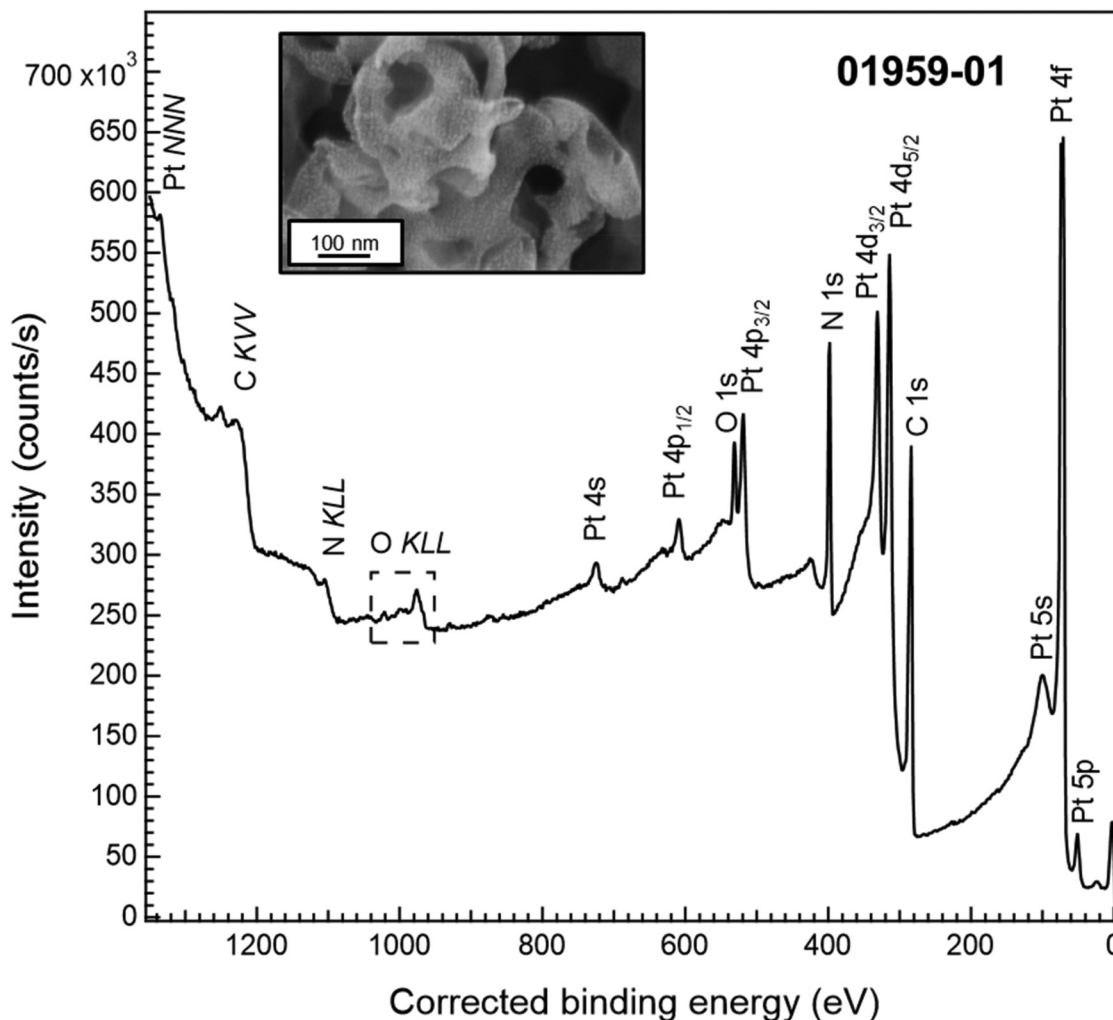
01959-01

20 August 2024 12:16:47

Accession #:	01959-01
■ Specimen:	gCN-Pt(Ar)
■ Technique:	XPS
■ Spectral Region:	Survey
Instrument:	ThermoFisher Scientific Escalab Xi+
Excitation Source:	Al K_α monochromatic
Source Energy:	1486.6 eV
Source Strength:	200 W
Source Size:	0.5 × 0.5 mm^2
Analyzer Type:	Spherical sector analyzer
Incident Angle:	58°
Emission Angle:	0°
Analyzer Pass Energy:	150 eV
Analyzer Resolution:	1.5 eV
Total Signal Accumulation Time:	204.2 s
Total Elapsed Time:	224.6 s
Number of Scans:	3
Effective Detector Width:	1.5 eV

■ **Accession #:** 01959-02
■ **Specimen:** gCN-Pt(Ar)
■ **Technique:** XPS
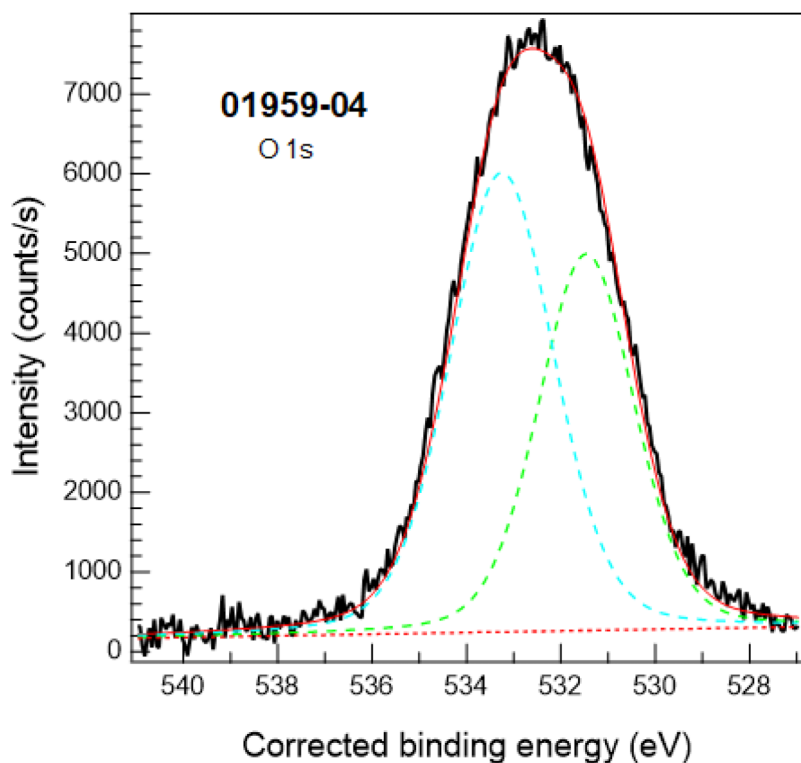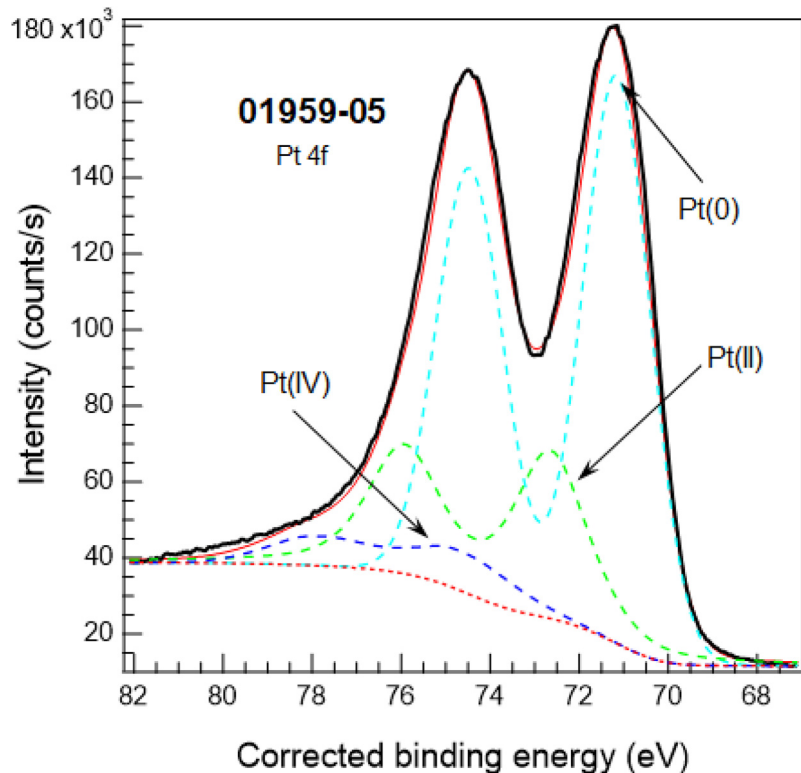■ **Spectral Region:** C 1*s*

Instrument: ThermoFisher Scientific Escalab Xi+
Excitation Source: Al K_α monochromatic
Source Energy: 1486.6 eV
Source Strength: 200 W
Source Size: 0.5 × 0.5 mm^2
Analyzer Type: Spherical sector
Incident Angle: 58°
Emission Angle: 0°
Analyzer Pass Energy: 50 eV
Analyzer Resolution: 0.5 eV
Total Signal Accumulation Time: 95.3 s
Total Elapsed Time: 104.8 s
Number of Scans: 5
Effective Detector Width: 0.5 eV
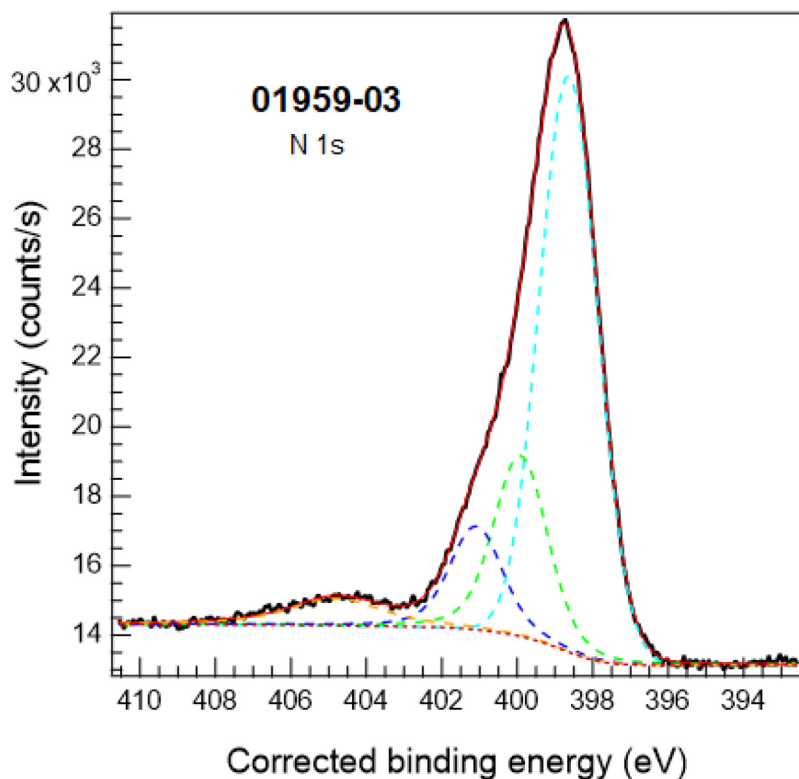
■ **Accession #:** 01959-03
■ **Specimen:** gCN-Pt(Ar)
■ **Technique:** XPS
■ **Spectral Region:** N 1*s*

Instrument: ThermoFisher Scientific Escalab Xi+
Excitation Source: Al K_α monochromatic
Source Energy: 1486.6 eV
Source Strength: 200 W
Source Size: 0.5 × 0.5 mm^2
Analyzer Type: Spherical sector
Incident Angle: 58°
Emission Angle: 0°
Analyzer Pass Energy: 50 eV
Analyzer Resolution: 0.5 eV
Total Signal Accumulation Time: 90.3 s
Total Elapsed Time: 99.3 s
Number of Scans: 5
Effective Detector Width: 0.5 eV

20 August 2024 12:16:47

■ **Accession #:** 01959-04
■ **Specimen:** gCN-Pt(Ar)
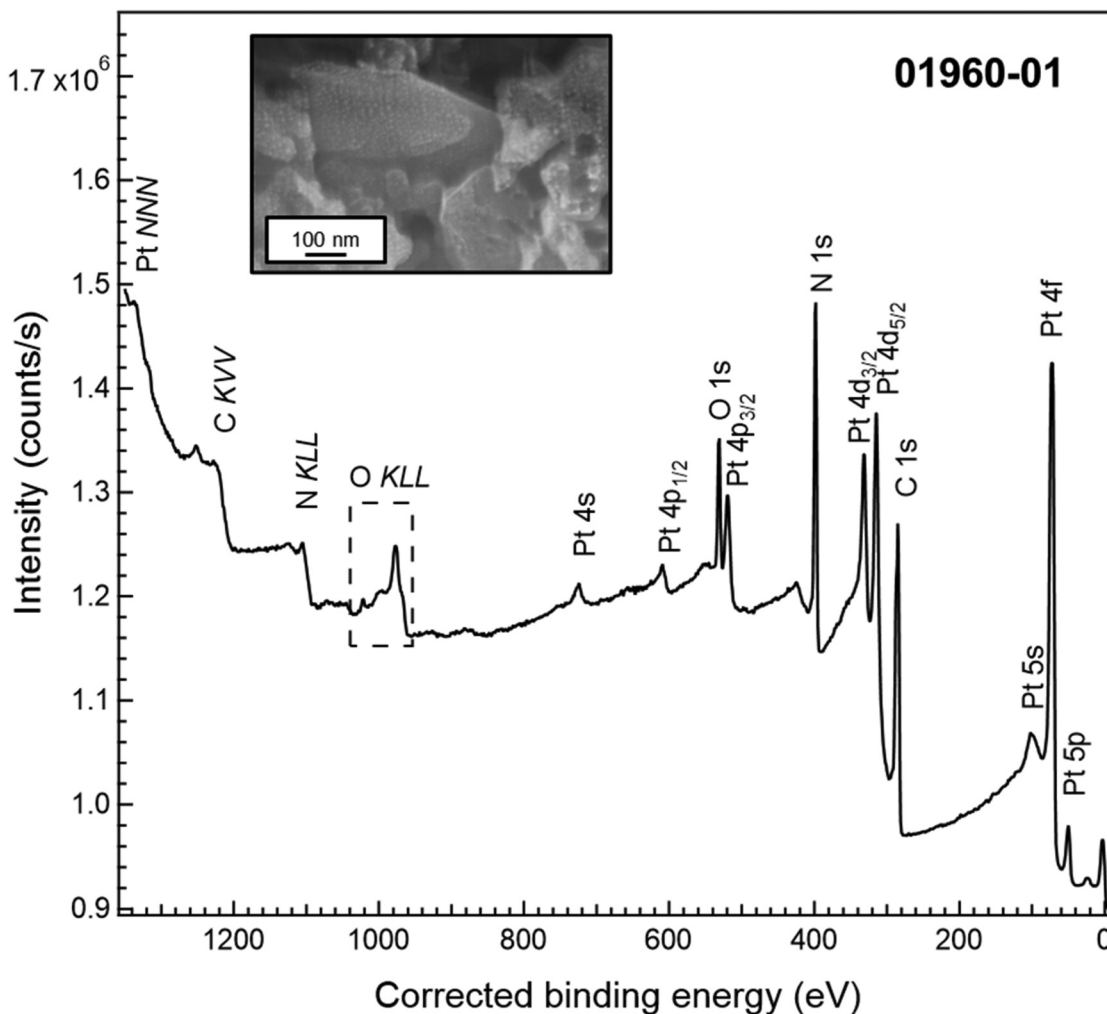■ **Technique:** XPS
■ **Spectral Region:** O 1*s*

Instrument: ThermoFisher Scientific Escalab Xi+
Excitation Source: Al K_α monochromatic
Source Energy: 1486.6 eV
Source Strength: 200 W
Source Size: 0.5 × 0.5 mm^2
Analyzer Type: Spherical sector
Incident Angle: 58°
Emission Angle: 0°
Analyzer Pass Energy: 50 eV
Analyzer Resolution: 0.5 eV
Total Signal Accumulation Time: 160.4 s
Total Elapsed Time: 176.4 s
Number of Scans: 8
Effective Detector Width: 0.5 eV

■ **Accession #:** 01959-05
■ **Specimen:** gCN-Pt(Ar)
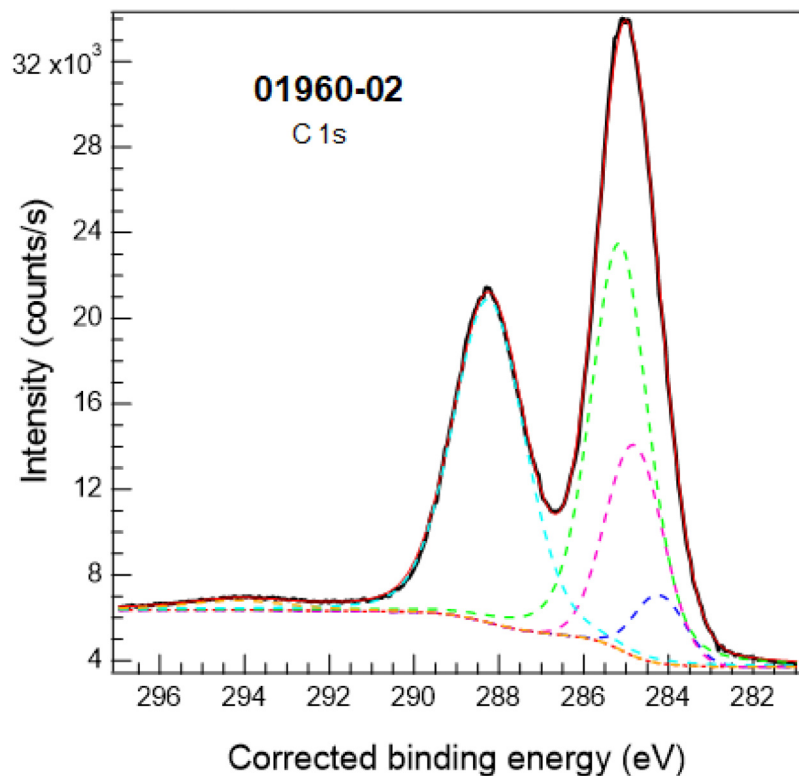■ **Technique:** XPS
■ **Spectral Region:** Pt 4*f*

Instrument: ThermoFisher Scientific Escalab Xi+
Excitation Source: Al K_α monochromatic
Source Energy: 1486.6 eV
Source Strength: 200 W
Source Size: 0.5 × 0.5 mm^2
Analyzer Type: Spherical sector
Incident Angle: 58°
Emission Angle: 0°
Analyzer Pass Energy: 50 eV
Analyzer Resolution: 0.5 eV
Total Signal Accumulation Time: 150.3 s
Total Elapsed Time: 165.3 s
Number of Scans: 6
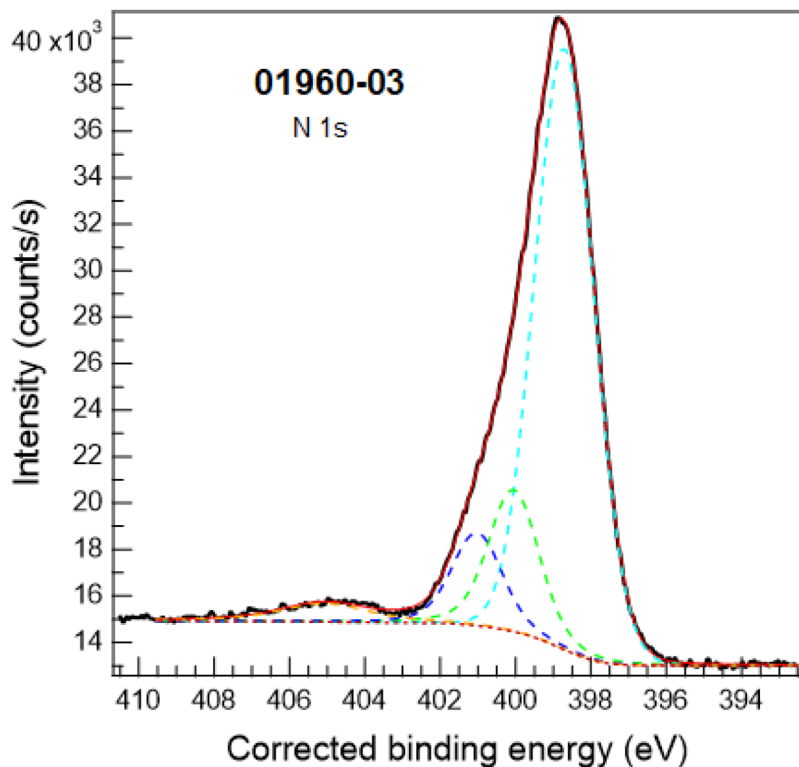Effective Detector Width: 0.5 eV

20 August 2024 12:16:47

Accession #:	01960-01
■ Specimen:	gCN-Pt(air)
■ Technique:	XPS
■ Spectral Region:	Survey
Instrument:	ThermoFisher Scientific Escalab Xi+
Excitation Source:	Al K_α monochromatic
Source Energy:	1486.6 eV
Source Strength:	200 W
Source Size:	0.5×0.5 mm^2
Analyzer Type:	Spherical sector analyzer
Incident Angle:	58°
Emission Angle:	0°
Analyzer Pass Energy:	150 eV
Analyzer Resolution:	1.5 eV
Total Signal Accumulation Time:	204.2 s
Total Elapsed Time:	224.6 s
Number of Scans:	3
Effective Detector Width:	1.5 eV

20 August 2024 12:16:47

■ **Accession #:** 01960-02
■ **Specimen:** gCN-Pt(air)
■ **Technique:** XPS
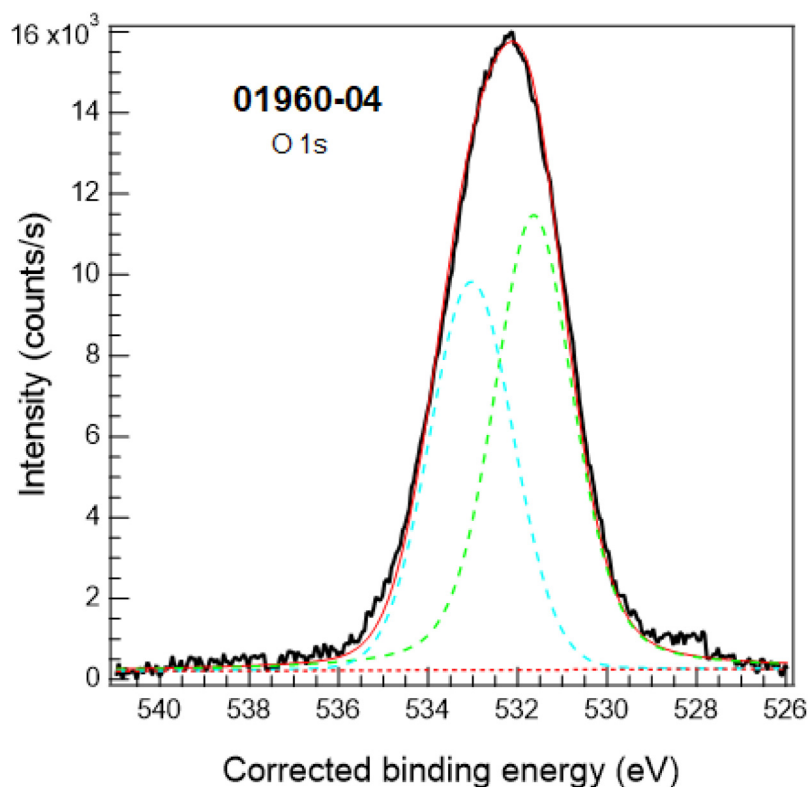■ **Spectral Region:** C 1s

Instrument: ThermoFisher Scientific Escalab Xi+
Excitation Source: Al K_α monochromatic
Source Energy: 1486.6 eV
Source Strength: 200 W
Source Size: 0.5 × 0.5 mm^2
Analyzer Type: Spherical sector
Incident Angle: 58°
Emission Angle: 0°
Analyzer Pass Energy: 50 eV
Analyzer Resolution: 0.5 eV
Total Signal Accumulation Time: 95.3 s
Total Elapsed Time: 104.8 s
Number of Scans: 5
Effective Detector Width: 0.5 eV

■ **Accession #:** 01960-03
■ **Specimen:** gCN-Pt(air)
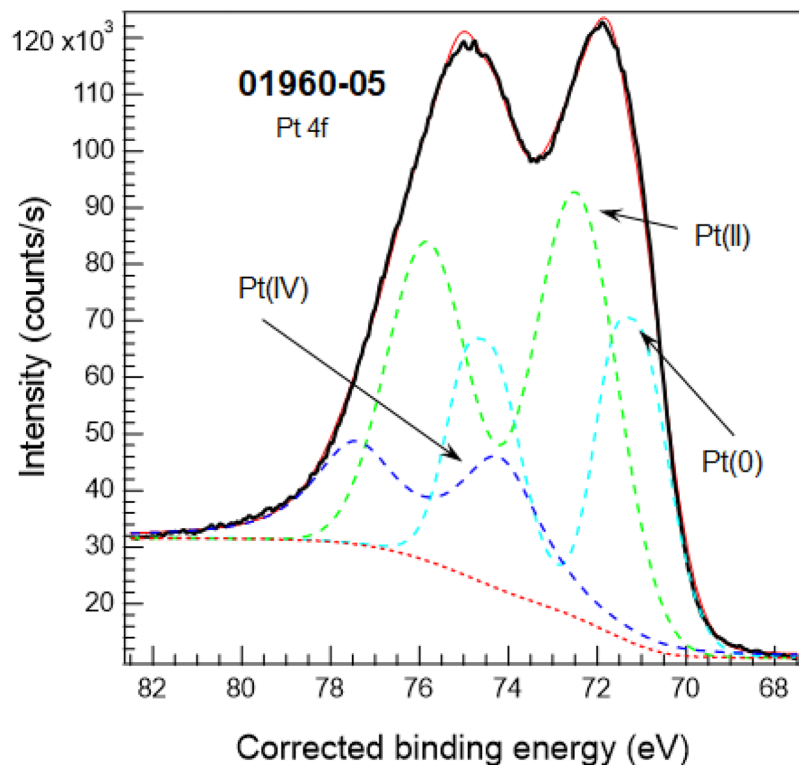■ **Technique:** XPS
■ **Spectral Region:** N 1s

Instrument: ThermoFisher Scientific Escalab Xi+
Excitation Source: Al K_α monochromatic
Source Energy: 1486.6 eV
Source Strength: 200 W
Source Size: 0.5 × 0.5 mm^2
Analyzer Type: Spherical sector
Incident Angle: 58°
Emission Angle: 0°
Analyzer Pass Energy: 50 eV
Analyzer Resolution: 0.5 eV
Total Signal Accumulation Time: 90.3 s
Total Elapsed Time: 99.3 s
Number of Scans: 5
Effective Detector Width: 0.5 eV

20 August 2024 12:16:47

■ **Accession #:** 01960-04
■ **Specimen:** gCN-Pt(air)
■ **Technique:** XPS
■ **Spectral Region:** O 1s

Instrument: ThermoFisher Scientific Escalab Xi+
Excitation Source: Al K_α monochromatic
Source Energy: 1486.6 eV
Source Strength: 200 W
Source Size: 0.5 × 0.5 mm^2
Analyzer Type: Spherical sector
Incident Angle: 58°
Emission Angle: 0°
Analyzer Pass Energy: 50 eV
Analyzer Resolution: 0.5 eV
Total Signal Accumulation Time: 160.4 s
Total Elapsed Time: 176.4 s
Number of Scans: 8
Effective Detector Width: 0.5 eV

■ **Accession #:** 01960-05
■ **Specimen:** gCN-Pt(air)
■ **Technique:** XPS
■ **Spectral Region:** Pt 4f

Instrument: ThermoFisher Scientific Escalab Xi+
Excitation Source: Al K_α monochromatic
Source Energy: 1486.6 eV
Source Strength: 200 W
Source Size: 0.5 × 0.5 mm^2
Analyzer Type: Spherical sector
Incident Angle: 58°
Emission Angle: 0°
Analyzer Pass Energy: 50 eV
Analyzer Resolution: 0.5 eV
Total Signal Accumulation Time: 150.3 s
Total Elapsed Time: 165.3 s
Number of Scans: 6
Effective Detector Width: 0.5 eV

20 August 2024 12:16:47